Supporting Information

D'Errico et al. 10.1073/pnas.1016354108

SI Methods

Mice. Nude mice for the xenograft experiments were obtained from the Jackson Laboratory. A total of 100 μL of colorectal cancer cells suspension (1×10^7 HT29) was s.c. injected to the subscapular region of an athymic mouse. All of the animals were randomly divided into two groups, each group containing 10 mice as follows: AdLacZ group (negative control) and AdPGC1α group (treatment group). Subsequently, 100 μL of a suspension of adenovirus (10^9 pfu) was administered directly into the tumor-bearing mice in each group every 4 d for a total of five injections per mouse. Long diameter (a) and short diameter (b) were measured every 3–4 d, and volumes (V) of the tumors were calculated according to the formula $V = ½ \cdot a \cdot b^2$, and a tumor growth curve was drawn. At day 2 following the final treatment, all of the mice were killed, and tumors were harvested for further analysis.

The iPGC1α transgenic mice were generated by injecting into the pronuclei of the fertilized eggs of the FVB/N mice the transgene digested with HpaI. To generate the pSKvillin PGC1α, first hPGC1α (2.4 kb) fragment with XhoI and SacII restriction sites was generated by PCR from pcDNA4 myc PGC1α plasmid (Addgene). Then the fragment was subcloned at the XhoI and SacII restriction sites downstream from the villin promoter region of the pSKVillin plasmid (kindly provided by Deborah Gumucio, University of Michigan Medical School). Mice carrying the transgene were identified by PCR of genomic DNA to confirm the presence of an hPGC1α coding sequence. Stomach, liver, jejunum, duodenum, ileum, and colon of transgenic mice were dissected and prepared for total RNA extraction and immunohistochemistry to evaluate the specific intestinal expression of transgene under the villin promoter control. iPGC1α $Apc^{Min/+}$ mice were generated by crossing iPGC1α transgenic mice with C57BL/6-$Apc^{Min/+}$ mice (Jackson Laboratory).

A straight knockout strategy, deleting exons 3–5, was used to target the *PGC1α* locus to generate mice carrying knockout alleles at this site (Fig. S4*A*). The targeting vector was built using homologous recombination in bacteria BHR. A C57 mouse BAC, RP23-385G21, served as a template for the extraction of homology arms of the targeting vector (Table S1). The 10.4-kb targeting vector, *PGC1α* Δex3–5, contained a floxed neomycin phosphotransferase, Neo, selectable marker cassette replacing sequences from intron 2 to intron 5. After linearization, the targeting construct was electroporated into AZX1, a C57BL/6JOlaHsd-derived ES cell line. PCR screens and Southern blot analyses revealed that three of 400 G418-resistant clones had undergone the desired homologous recombination. One of these clones was expanded and injected into Balb/cOlaHsd blastocysts to generate chimeric mice. Chimeric males were bred to C57BL/6JOlaHsd females, and black-coated offspring were genotyped, using a forward primer (F1) in intron 2 outside the short-arm homology combined with a reverse Neo-specific primer (R1), giving a PCR product of 2,508 bp.

Heterozygous *PGC1α* Δex3–5 floxed Neo mice were bred to a constitutive Cre-deleter strain of mice to generate the heterozygous *PGC1α* Δex3–$5^{+/-}$ mice lacking the Neo resistance cassette and leaving a single LoxP site at the deletion junction of intron 2 and 5. These mice were genotyped by using a forward primer (F2) in intron 2 and a reverse primer (R2) in intron 5. These primers gave a PCR product of 458 bp for the Cre-recombined (deleted) allele and a 5.5-kb PCR product for the WT allele. Heterozygous *PGC1α*$^{+/-}$ littermate mice were then intercrossed to generate homozygous *PGC1α*$^{-/-}$ mice. Liver cDNA was prepared from *PGC1α*$^{+/+}$, *PGC1α*$^{+/-}$, and *PGC1α*$^{-/-}$ mice, and after cDNA synthesis, RT-PCR was run to check for the presence or absence of *PGC1α* transcripts. To routinely genotype mice, a triple-primer (F2, F3, R2) PCR producing a shorter WT band was used.

For the chemical-induced colitis carcinogenesis model (1), 10 pathogen-free 16-wk-old male WT FVBN mice and i*PGC1α* transgenic mice on a pure FVBN background were injected i.p. with 12 mg/kg body weight of AOM dissolved in saline. Five days later, 3% DSS was given in the drinking water over 5 d, followed by 16 d of regular water. This cycle was repeated three times, and body weight was recorded at the end of each cycle. The same protocol was performed in ten 6-wk-old male WT C57B6/J and corresponding PGC1α$^{-/-}$ on the same pure C57B6/J background strain. Macroscopical inspection, histological analysis, and total RNA extraction were performed at the end of the protocol. Briefly, colons were thawed in 2.5% formalin solution at room temperature, fixed in 70% ethanol at 4 °C for 30 min, and stained with 0.2% methylene blue for 2 min. Stained colons were transferred to 2.5% formalin solution for up to 1 h (2) and then examined in their entirety under a light microscope. The number and size of tumors was recorded.

All mice were housed with a standard diet provided ad libitum, and examined daily. Genotyping was done using DNA extracted from tail biopsies of 1- to 2-wk-old pups, and new breeding harems of 4- to 5-wk-old mice were established to expand the population. All of the experiments presented in this study have been carried out in male mice. The ethics committee of the Consorzio Mario Negri Sud approved this experimental setup, which was also certified by the Italian Ministry of Health in accordance with internationally accepted guidelines for animal care.

FAP Patients. Unrelated FAP patients were recruited for the study after approval by the ethics committee of the University "G. D'Annunzio" of Chieti. Written informed consent was obtained from each patient before mutation analysis and tissue harvesting. All the included cases presented with a classical FAP phenotype and harbored pathogenetic germline *APC* mutations. Genomic DNA was isolated from at least two independently drawn blood samples using QIAamp DNA Blood (QIAGEN). The coding sequence and intron-exon borders of *APC* were analyzed by a combination of PCR-based techniques that included heteroduplex analysis on agarose minigel (HAAM) for recurring mutations, in vitro synthesized protein assay of exon 15, single-strand conformational polymorphism analysis of the remaining exons, and denaturing HPLC (DHPLC; Wave 1100; Transgenomic, Inc.) of *APC* exons 1–15 followed by sequencing (3). All mutations were confirmed in at least two different blood samples.

Transient Transfection and Adenoviral Constructs. Where indicated, 1.5×10^6 cells per well were seeded in six-well plates and transfected with 4 μg of pCDNA-PGC1α (Addgene) or empty pCDNA4 (Invitrogen) or pCDNA4-GFP using 4 μL of Lipofectamine 2000 (Invitrogen), 250 μL of Opti-MEM (Invitrogen), and 1.5 mL of medium without antibiotic supplementation. After 48 or 72 h, cells were analyzed. Human PGC1α adenovirus (hAdPGC1α) was generated using the Viral Power Adenoviral Expression System (Invitrogen). Briefly, the hPGC1α coding sequence was PCR amplified and subcloned from the pcDNA4myc PGC1α plasmid into the pENTR4 shuttle vector using SalI and NotI restriction sites. Then, pENTR4h PGC1α plasmid was recombined with the destination vector pAd/CMV/V5-DEST to generate an adenovector containing hPGC1α under the control of

the human cytomegalovirus promoter. The adenovector coding β-galactosidase under the control of the human cytomegalovirus promoter (pAd/CMV/V5-GW/lacZ) was purchased from Invitrogen. Then, adenovectors were linearized with Pac I restriction enzyme and the digested products, after purification with QIAEX II Gel Extraction Kit (Qiagen), were used to transfect 293A cells (Invitrogen) with Lipofectamine 2000 (Invitrogen) to generate the corresponding adenoviruses. The viruses were propagated into 293A cells. Adenoviral titer was determined by real-time qPCR with specific primers (4). Crude viral lysate stocks were stored at −80 °C until use.

Generation of HT29ρ0 Cells. The HT29 cell line was grown in DMEM (high glucose) supplemented with 10% (vol/vol) FBS, 1% (vol/vol) L-glutamine, 1% (vol/vol) penicillin, and streptomycin at 37 °C in a humidified atmosphere of 5% CO_2. The mtDNA-depleted HT29ρ0 cells cell line used in the present work was generated by ethidium bromide treatment (5). Briefly, HT29 cells were cultured for ∼8 wk in the same growth medium without antibiotics and supplemented with 0.4 μg/mL of ethidium bromide (EtBr), 50 μg/mL uridine, and 100 μg/mL pyruvate. After checking for the complete absence of mtDNA, the cells were cultured in the standard HT29 growth medium supplemented with 50 μg/mL uridine and 100 μg/mL pyruvate.

Detection of mtDNA by PCR Analysis. To verify the complete removal of the mtDNA, the total genomic DNA of the HT29ρ0 cells was isolated (JETquick Kit; GENOMED) and used as a template in a multiplex PCR test. The genomic DNA from HT29 WT and 143Bρ0 cell lines were used as positive and negative controls, respectively. The multiplex PCR was carried out with primers for the mitochondrial cyt *b* gene (forward-5′tacaaccacgaccaatgatatgaaa3′ and reverse-5′aggttttcatcatctccggtttacaag 3′) and the nuclear actin gene (forward-5′tgactgactcctcatgaagatc3′ and reverse-5′ccgtcaggcagctcgtagctct3′). The annealing temperature was 55 °C for 30 cycles with an elongation time of 45 s.

Western Blot Analysis. For Western blots, equal amounts of total cellular proteins (20–30 μg) were separated on a 13% SDS/PAGE and transferred onto nitrocellulose membrane. Membranes were then blocked with 5% nonfat milk in 0.1% TBS Tween-20 and probed with specific antibodies against mitochondrial-encoded COXI gene (Molecular Probes) and the nuclear-encoded β-actin (Sigma). Membranes were then incubated with HRP-conjugated secondary antibodies (Bio-Rad) and developed with a chemiluminescent reagent (Euroclone).

Measurement of Mitochondrial Respiration Rates in Intact Cells. The respiratory activity of intact cells was measured polarographically with a Clark-type oxygen electrode in a water-jacketed chamber (Hansatech Instruments), magnetically stirred at 37 °C, essentially as previously described (6). Briefly, exponentially growing cells were collected by trypsinization and centrifugation, and then transferred into the polarographic chamber at 4–6 × 10^6 cells/mL in TD buffer [0.137 M NaCl, 5 mM KCl, 0.7 mM Na_2HPO_4, 25 mM Tris·HCl (pH 7.4)], previously air equilibrated at 37 °C. The respiration rates by endogenous substrates were read directly (basal endogenous respiration) after addition of 2,4-dinitrophenol (DNP) to 60 μM (uncoupled maximal endogenous respiration) of sodium ascorbate (10 mM) + TMPD (0.4 mM; Fluka/Sigma-Aldrich) as artificial membrane-permeant electron donors to COX, in the presence of the upstream respiratory chain inhibitor antimycin A (40 nM). Due to the biphasic response of the cellular respiration to DNP (7), a DNP titration was carried out in HT29 cells to choose the optimal DNP concentration as the minimal one resulting in the maximal stimulation of the respiration rate. COX_{Rmax} was calculated as described (6).

Determination of Mitochondrial Enzyme Activities. Cyt *c* oxidase and citrate synthase enzyme activities were measured spectrophotometrically in digitonin-permeabilized cell lysates as previously described (8). For the preparation of the HT29 cell lysates, a digitonin titration was carried out to choose the optimal amount of detergent (15 μg/10^6 cells) as the one eliciting the highest succinate-dependent uncoupled respiration rate (7). Protein concentration was determined according to the Bradford method, using BSA as a standard.

EUK134 Treatment. EUK134 was purchased from Cayman. This salen–manganese compound is a SOD/catalase mimetic (9). A primary stock of EUK134 48 mM in DMSO was prepared and diluted in DMEM to a final concentration of 2.5 μM. Briefly, 1 × 10^6 HT29 cells were seeded in six-well plates and infected with 100 MOI AdPGC1α and AdLacZ as a control for 48 h. EUK134 and DMSO (vehicle) 2.5 μM diluted in DMEM was added to the culture medium 2 h before adenoviral infection and every 24 h for the entire experimental procedure. Cells were then harvested and analyzed for ROS accumulation and Annexin V-FACS analysis as described. In nude mice xenograft experiments, EUK134 and DMSO (vehicle) 2.5 μM in DMEM were administrated into tumors 2 h before adenoviral treatment during the entire procedure.

Cell Death Assay. A total of 0.6 × 10^6 cells/well were seeded in a 12-well plate and infected with AdPGC1α; after 72 h, 10^4 cells were seeded in a 96-well plate and processed according to the Cell Death Detection ELISA Plus (Roche Diagnostic) manufacturer's protocol. The quantification of nucleosomes was carried out through a photometric analysis measuring at 405 nm (reference wavelength ∼490 nm). The specific enrichment of nucleosomes released into the cytoplasm was calculated using the following formula: enrichment factor = absorbance of the sample (PGC1α)/absorbance of the corresponding control (LacZ). Data have been also normalized on total protein concentration.

Cell Proliferation Assay. The amount of proliferating cells was evaluated using the Cell Proliferation ELISA Kit (Roche Diagnostics). A total of 10^4 HT29 cells per well (six samples for each condition) were seeded in 96-well culture dishes and infected with 200 MOI of AdPGC1α and AdLacZ for 48 h. BrdU was then added to the culture medium 24 h before cell harvesting. The proliferating cells were evaluated by measuring the incorporation of BrdU during DNA synthesis colorimetrically at 370 nm. Proliferation was calculated using the following formula: proliferation = absorbance of the sample (PGC1α)/absorbance of the corresponding control (LacZ). Data have been normalized to total protein concentration.

Measurement of mtDNA by RT-PCR Analysis. After PGC1α overexpression, mtDNA was quantified by real-time PCR. Real-time qPCR primers were designed using Primer Express software. Briefly, cells were harvested and total DNA was extracted using the DNeasy Tissue Kit (Qiagen) according to the manufacturer's instruction. Sixty nanograms of total DNA were used in real-time PCR analysis performed in 96-well optical reaction plates using an ABI 7500HT machine (Applied Biosystems). The PCR was carried out with primers for the mitochondrial cyt *c* gene (forward-5′cctgcgactccttgacgttg3′ and reverse-5′agcggtgaaagtggtttggtt3′) and the nuclear actin gene (forward-5′ tcacccacactgtgcccatctacga 3′ and reverse-5′cagcggaaccgctcattgccaatgg3′). PCR assays were conducted in triplicate wells for each sample. Baseline values of amplification plots were set automatically, and threshold values were kept constant to obtain normalized cycle times and linear regression data. The following reaction mixture per well was used: 10 μL Power SYBR Green (Applied Biosystems),

2.4 μL of primers at the final concentration of 150 nM, 4.6 μL sterile water, and 3 μL total DNA (60 ng). For all experiments, the following PCR conditions were used: denaturation at 95 °C for 10 min, followed by 40 cycles at 95 °C for 15 s, then at 60 °C for 60 s. Quantitative normalization of mtDNA in each sample was performed using actin as an internal control.

Measurements of ROS Levels. The intracellular ROS levels were determined using CM-H_2DCFDA (Molecular Probes, Invitrogen) after 48 h of AdPGC1α and AdLacZ infection. For these experiments, cells were incubated with PBS and 5 μM CM-H_2DCFDA. As a negative control, cells were incubated with PBS and vehicle (DMSO). As a positive control, cells were incubated with PBS, 5 μM CM-H_2DCFDA, and 100 μM H_2O_2. After a 1-h incubation period, cells were trypsinized, washed, and resuspended in PBS. The levels of fluorescence were immediately detected using flow cytometry.

Immunocytochemistry. After different treatments, cells were fixed in 4% paraformaldehyde in PBS for 10 min at room temperature, and standard immunofluorescence protocols were used. Briefly, after fixation, cells were washed with 0.01 M PBS (pH 7.4), incubated with blocking buffer (0.5% BSA, 0.05% saponin, 0.1 M NH_4Cl, 0.02% NaN_3) for 20 min at room temperature. Cells were then incubated with the primary antibody to penta-His (Qiagen) and cyt *c* (Abcam) for 30 min at room temperature to localize the antigen. In the transfection assay, we used the pcDNA4 myc PGC1α plasmid (Addgene). After three washes with PBS, cells were incubated with the secondary antibody Alexa 488 conjugated, Alexa 633 conjugated (1:400), and Hoecst 33258 (1:1,000; Sigma-Aldrich) to localize nuclei for 30 min at room temperature. Staining for Annexin V-Alexa 568 (Roche Diagnostics) and MitoTracker Red 580 (Invitrogen) were carried out according to the manufacturer's protocols. Briefly, for Annexin-V staining, cells were harvested, washed with PBS, and immediately incubated for 15 min at room temperature with Annexin V diluted 1:200 in incubation buffer [10 mM Hepes/NaOH (pH 7.4), 140 mM NaCl, 5 mM CaCl]. Cells were then washed with incubation buffer and fixed in 4% paraformaldehyde in PBS for 10 min at room temperature, and standard immunofluorescence protocols were used.

For Annexin V-FACS analysis, the Annexin V-FITC Apoptosis Detection Kit (Sigma) was used. Briefly, 1×10^6 HT29 cells were seeded in a six-well plate and infected with 100 MOI AdPGC1α and AdLacZ as a control for 48 h. Cells were than washed twice with PBS and resuspended in 1× binding buffer (provided by the manufacturer) at a concentration of 1×10^6 cells/mL; 5 μL of Annexin V-FITC conjugate and 10 μL of propidium iodide solution were added to 500 μL of each cell suspension. After a 10-min incubation at room temperature (dark), the fluorescence of cells was immediately determined with a flow cytometer. The number of cells positive to the Annexin V-FITC conjugate staining was expressed as a percentage.

For MitoTracker Red 580 staining, 100 nM MitoTracker Red 580 solution in phenol red-free medium was added to the cells and incubated for 45 min at 37 °C. Cells were then washed with fresh medium and fixed in 4% paraformaldehyde in PBS for 10 min at room temperature, and standard immunofluorescence protocols were used. Cells were finally washed with PBS and the coverslips mounted with Mowiol™ (Calbiochem). For images examined with the Zeiss LSM 510 confocal microscope (1,260× magnification), optical sections were obtained with a 63× oil immersion objective at a definition of 1,024 × 1,024 pixels and a pinhole diameter of 1 airy unit for each emission channel.

Fatty Acid Oxidation Assay. Palmitic acid oxidation was assayed as described (10). Cells were plated at a density of 0.5×10^6 cells per well in a six-well plate and infected with AdPGC1α (AdlacZ as control). After treatments, cells were cultured in 2 mL of DMEM containing 2% free fatty acids BSA, 0.3 mM palmitic acid, and 5 μCi of [9,10-^{3}H]palmitic acid (PerkinElmer). After 2 h, palmitic oxidation was assessed by measuring ^3H_2O produced in the incubation medium. The media (1 mL) were extracted by the addition of 5 mL of methanol/chloroform (1:2, vol/vol) and 2 mL of 2 M KCl/HCl (1:1, vol/vol), followed by centrifugation at 3,000 × *g* for 15 min. ^3H_2O release in the aqueous phase was measured by liquid scintillation counting. Background ^3H_2O release, as measured in an aliquot of medium with [9,10-^{3}H]palmitic acid that was incubated without cells, was subtracted from experimental values. Values obtained for each sample were normalized on protein concentration and expressed as cpm per milligram protein × 10^{-3}.

Glycolysis Assay. Glycolysis was assayed as the rate of conversion of [5-^{3}H]glucose to [^{3}H]water ([^{3}H]water is liberated at the phosphoglucoisomerase step of glycolysis). Briefly, cell monolayers in 48-well dishes after 48 h of AdPGC1α and AdLacZ infection were washed twice in Krebs-Ringer solution containing 140 mM NaCl, 3.6 mM KCl, 1.5 mM $CaCl_2$, 0.5 mM $MgSO_4$, 0.5 mM Na_2HPO_4, 2 mM NaH_2CO_3, 10 mM Hepes (pH 7.4), and 0.07% BSA, and incubated at 37 °C in 0.3 mL of the same medium supplemented with glucose at 25 mM and 0.5 μCi of tracer [5-^{3}H]glucose (PerkinElmer). After a 60-min incubation, the medium was aspirated and centrifuged at 4 °C to remove cell debris. To separate the [^{3}H]water produced from radioactive glucose, columns of Dowex in the borate form were loaded with samples of 0.2 mL of medium and eluted with 2 mL of water (11). The data were expressed as cpm per cell number × 10^2.

Protein Extraction. Cells were scraped from six-well plates in ice-cold PBS and then centrifuged for 5 min at 956 × *g* at 4 °C. Supernatant was discarded and pellets resuspended in 200 μL lysis buffer composed of 80% RIPA buffer [50 mM Tris·HCl (pH 8.0) with 150 mM sodium chloride, 1.0% Igepal CA-630 (Nonidet P-40), 0.5% sodium deoxycholate, 0.1% SDS (Sigma-Aldrich), and 20% protease inhibitor (Roche Diagnostic)]. After 15 min in ice, samples were centrifuged for 10 min at 12,000 rpm at 4 °C.

Immunohistochemistry. Tissue specimens were fixed in 10% formalin for 12–24 h, dehydrated, and paraffin embedded. Standard immunohistochemical procedures were performed. Briefly, 5-μm–thick sections were treated with 3% hydrogen peroxide for 5 min to quench endogenous peroxidase, and subjected to antigen retrieval by boiling the slides in antigen-unmasking solution (Vector Laboratories) for 20 min according to the manufacturer's instructions. Sections were sequentially incubated for 30 min at room temperature in 50% nonimmune serum (from the host animal in which the secondary antibody was raised) in PBS and overnight at 4 °C with the primary antibodies (rabbit polyclonal Ki67 and MCAD from AbCam; rabbit PGC1α from Santa Cruz, Calbiochem, Abcam, and Bethyl; rabbit polyclonal CAT and SOD2 from AbCam; and mouse monoclonal Anti-OxPhos Complex IV Subunit I from Invitrogen). Sections were then washed 10 min in PBS and incubated for 30 min at room temperature with the secondary biotinylated antibody (Vector Laboratories). After several washing steps with PBS (three washes, 5 min each), sections were incubated with the avidin-biotin complex (Vector Laboratories) for 30 min at room temperature. After washing in PBS, the peroxidase reaction was developed by incubation with diaminobenzidine (DAB; Sigma-Aldrich). Counterstaining was carried out with methylene blue (Sigma-Aldrich). For negative controls, 1% nonimmune serum in PBS replaced the primary antibodies.

For TUNEL assay, paraffin-embedded sections were deparaffinizated by heating for 4 h at 60 °C, and then hydrated with the

following solution: twice in xylene bath for 5 min, and then for 5 min in absolute ethanol, 96% ethanol, 80% ethanol, 70% ethanol, and double-distilled water. The apoptotic cells were stained using the In Situ Cell Death Detection Kit, Fluorescein (Roche Diagnostic) according the manufacturer's protocol. Data obtained on TUNEL assays have been quantified through the image processing and analysis tools in the Zeiss LSM 510 confocal microscope.

Electron Microscopy. Ileum and colon tissues were dissected, washed with PBS, and fixed in 1% glutaraldehyde dissolved in 0.2 M Hepes buffer (pH 7.4) for 30 min at room temperature. The specimens were then postfixed for 2 h in OsO_4. After dehydration in graded series of ethanol and propilenoxide, the cells were embedded in Epon 812 (Fluka) and polymerized at 60 °C for 72 h. Thin sections were cut at the Leica EM UC6 and counterstained with uranyl acetate and lead citrate. EM images were acquired from thin sections using a Philips Tecnai 12 electron microscope equipped with an Ultra View CCD digital camera (Philips).

Histochemical Procedures. Frozen intestines from transgenic mice and tumors from xenograft mice were included in O.C.T. Compound Tissue-Tek (Electron Microscopy Sciences). Cryostat sections of 20 μm were cut on a cryostat at a cabinet temperature of −20 °C and mounted onto glass slides.

COX staining was performed according to Gonzales-Lima (12). Sections were preincubated for 10 min in Tris buffer (0.05 M, pH 7.6) solution containing 0.0275% cobalt chloride, 10% sucrose, and 0.5% DMSO. Sections were then incubated for 2 h in PBS containing 0.05% DAB, 0.0075% cyt *c*, 5% sucrose, 0.002% catalase, and 0.25% DMSO at 37 °C. Sections were than immersed in PBS with 4% formaldehyde, dehydrated, and covered with a coverslip. To detect ROS, 10-μm cryostat sections were incubated in a medium prepared according to Kerver et al. (13) containing 12.5 mM DAB, 5 mM $MnCl_2$, and 40 mM Co Cl_2 dissolved in 10%, in 100 mM Tris-maleate buffer (pH 8.0) at 37 °C. After 30 min incubation, the sections were rinsed in hot distilled water (60 °C) to stop the reaction and to remove the viscous incubation medium. Data obtained on ROS and COX have been quantified through the image processing and analysis tools from ImageJ version 1.43 (http://rsbweb.nih.gov/ij/).

RNA Extraction. Total RNA was isolated by TRIzol reagent (Invitrogen) following the manufacturer's instructions. To avoid possible DNA contaminations, RNA was treated with DNase I (Ambion). RNA purity was checked by spectrophotometer and RNA integrity by examination on agarose gel electrophoresis. cDNA was synthesized retrotranscribing 4 μg of total RNA in a total volume of 100 μL using a High Capacity DNA Archive Kit (Applied Biosystems) per the manufacturer's instructions.

Quantitative Real-Time PCR. Real-time qPCR primers were designed using Primer Express software. PCR assays were performed in 96-well optical reaction plates using an ABI 7500HT machine (Applied Biosystems). PCR assays were conducted in triplicate wells for each sample. Baseline values of amplification plots were set automatically, and threshold values were kept constant to obtain normalized cycle times and linear regression data. The following reaction mixture per well was used: 10 μL Power SYBR Green (Applied Biosystems), 2.4 μL of primers at the final concentration of 150 nM, 4.6 μL RNase-free water, and 3 μL cDNA (60 ng). For all experiments, the following PCR conditions were used: denaturation at 95 °C for 10 min, followed by 40 cycles at 95 °C for 15 s then at 60 °C for 60 s. Quantitative normalization of cDNA in each sample was performed using cyclophillin as an internal control. Relative quantification was performed using the $\Delta\Delta C_T$ method (3). Validated primers for real-time PCR are available upon request.

Microarray. Microarray gene expression analysis was conducted on RNA extracted from the ileum of WT, PGC1α$^{-/-}$, and iPGC1α mice. Experiments were conducted using the Whole-Genome gene expression direct hybridization assay via Mouse Expression BeadChips on the iScan Illumina. The metabolic pathways differentially expressed in the three mouse models have been identified using DAVID software on the DAVID Bioinformatics Resources Web site (http://david.abcc.ncifcrf.gov/).

Statistical Analysis. All results are expressed as mean ± SEM. Data distribution and gene expression statistical analysis was performed using NCSS Statistical and Power Analysis Software 2007. Multiple groups were tested by one-way ANOVA followed by Fisher's least significant difference test for unpaired data. Comparisons of two groups were performed using a Student's *t* test followed by Mann–Whitney *U* test where appropriate. $P < 0.05$ was considered significant.

1. Popivanova BK, et al. (2008) Blocking TNF-alpha in mice reduces colorectal carcinogenesis associated with chronic colitis. *J Clin Invest* 118:560–570.
2. Myung SJ, et al. (2006) 15-Hydroxyprostaglandin dehydrogenase is an in vivo suppressor of colon tumorigenesis. *Proc Natl Acad Sci USA* 103:12098–12102.
3. Modica S, et al. (2010) The intestinal nuclear receptor signature with epithelial localization patterns and expression modulation in tumors. *Gastroenterology* 138: 636–648, 648, e1–e12.
4. Thomas MA, Lichtenstein DL, Krajcsi P, Wold WS (2007) A real-time PCR method to rapidly titer adenovirus stocks. *Methods Mol Med* 130:185–192.
5. King MP, Attardi G (1989) Human cells lacking mtDNA: Repopulation with exogenous mitochondria by complementation. *Science* 246:500–503.
6. Villani G, Attardi G (1997) In vivo control of respiration by cytochrome c oxidase in wild-type and mitochondrial DNA mutation-carrying human cells. *Proc Natl Acad Sci USA* 94:1166–1171.
7. Villani G, Greco M, Papa S, Attardi G (1998) Low reserve of cytochrome *c* oxidase capacity in vivo in the respiratory chain of a variety of human cell types. *J Biol Chem* 273:31829–31836.
8. Seibel P, et al. (2008) Cosegregation of novel mitochondrial 16S rRNA gene mutations with the age-associated T414G variant in human cybrids. *Nucleic Acids Res* 36: 5872–5881.
9. Rong Y, Doctrow SR, Tocco G, Baudry M (1999) EUK-134, a synthetic superoxide dismutase and catalase mimetic, prevents oxidative stress and attenuates kainate-induced neuropathology. *Proc Natl Acad Sci USA* 96:9897–9902.
10. Luo B, et al. (2007) Chronic hexosamine flux stimulates fatty acid oxidation by activating AMP-activated protein kinase in adipocytes. *J Biol Chem* 282:7172–7180.
11. Hammerstedt RH (1973) The use of Dowex-1-borate to separate 3HOH from 2-3H-glucose. *Anal Biochem* 56:292–293.
12. Gonzalez-Lima F, Jones D (1994) Quantitative mapping of cytochrome oxidase activity in the central auditory system of the gerbil: A study with calibrated activity standards and metal-intensified histochemistry. *Brain Res* 660:34–49.
13. Kerver ED, et al. (1997) In situ detection of spontaneous superoxide anion and singlet oxygen production by mitochondria in rat liver and small intestine. *Histochem J* 29: 229–237.

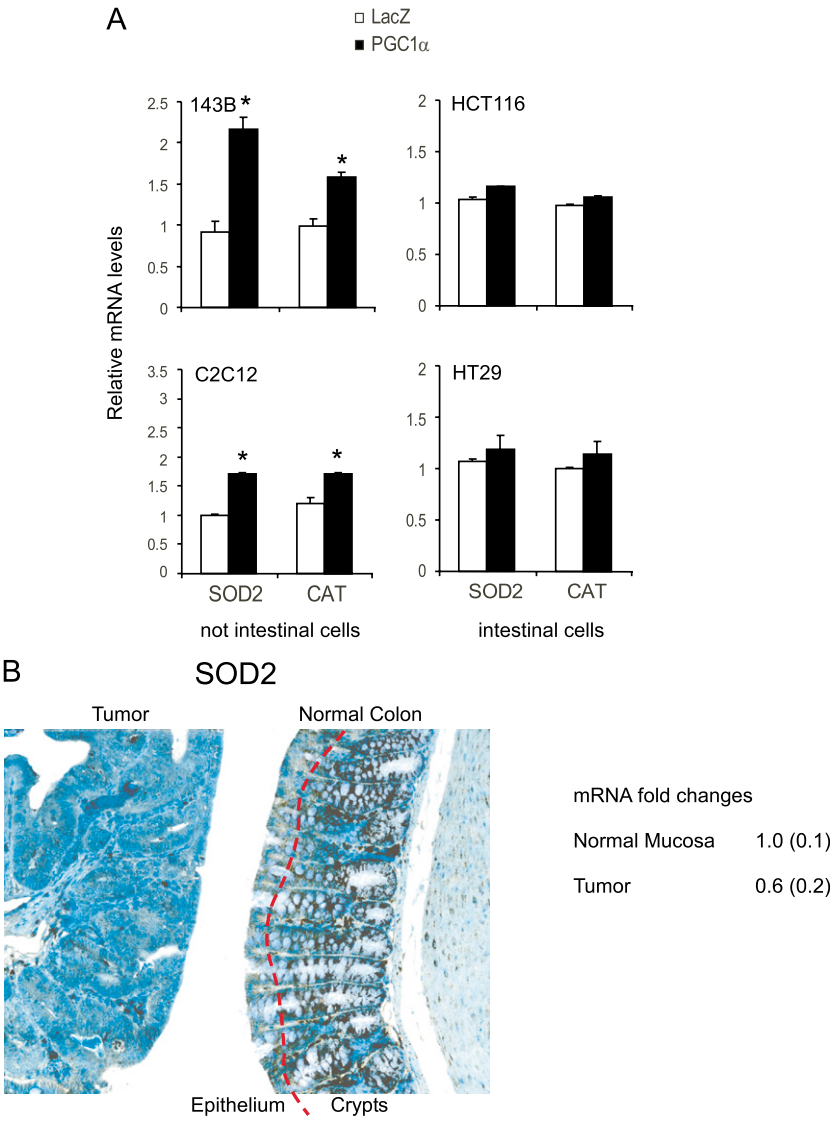

Fig. S1. ROS scavenger expression levels in HT29, HCT116, C2C12, and 143B. (*A*) mRNA levels of the antioxidant enzymes SOD2 and CAT from AdPGC1α- and AdLacZ-infected HT29, HCT116, C2C12, and 143B cells were evaluated after 48 h by real-time qPCR using cyclophilin as a reference gene. Results are expressed as mean ± SEM. (*B*) Immunohistochemical staining of SOD2 in a "rolled" colonic segment of $Apc^{Min/+}$ male mice. (*Left*) Tumor. (*Right*) Normal colon. SOD2 staining is restricted to the crypt compartment of the colonic mucosa with a major expression in the lower third of the crypts where stem cells reside. In contrast, SOD2 staining is almost absent in the apical epithelium of the normal colon and in the tumor. The decrease in SOD2 is presented as changes in mRNA levels between normal mucosa and tumors of $Apc^{Min/+}$ mice (real-time qPCR using cyclophilin as a reference gene).

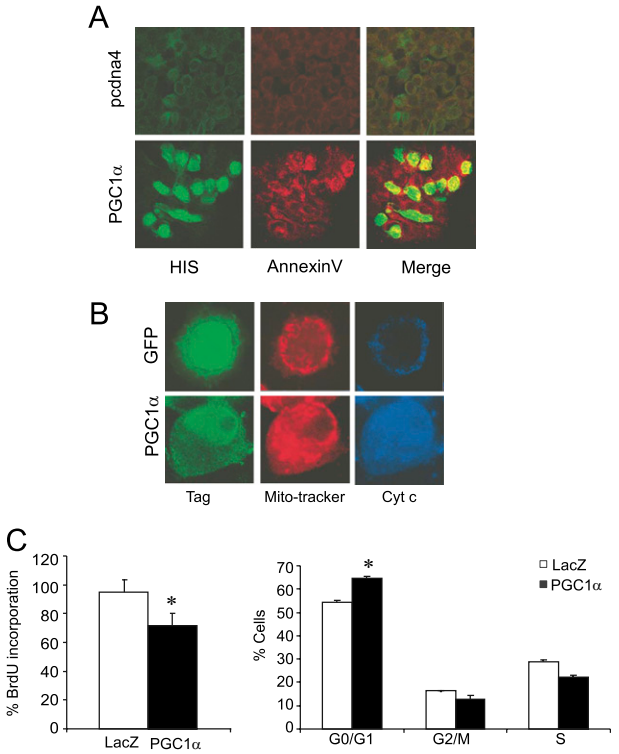

Fig. S2. PGC1α induces apoptosis in colorectal cancer cells. (*A*) Annexin V assay after PGC1α overexpression. HT29 cells were transfected with pCDNA-PGC1α or empty pCDNA4 as a control. After 48 h, cells were first incubated with Annexin V-Alexa (red) and fixed. Cells were incubated with the primary antibody to penta-His (green), and images acquired by confocal z-series covering the entire thickness of the cell. (*B*) Cyt *c* efflux. Cyt *c* (blue) is colocalized with the MitoTracker Red 580 (red) staining in control cells (GFP), whereas after PGC1α overexpression cyt *c* leaks out of the mitochondria into the cytosol. HT29 were transfected with pCDNA-PGC1α or pCDNA4-GFP as a control for 48 h and incubated with MitoTracker Red 580. Cells were then fixed, incubated with the primary antibody to penta-His (green) and to cyt *c* (blue), and images acquired by confocal z-series covering the entire thickness of the cell. (*C*) PGC1α overexpression affects cell proliferation and cell distribution throughout the cell cycle phases. HT29 cells were seeded and infected with AdPGC1α and AdLacZ for 48 h. The number of proliferating cells was evaluated by measuring the incorporation of BrdU during DNA synthesis colorimetrically at 370 nm. Data have been normalized on protein concentration and reported as a percentage. For cell cycle distribution of HT29 cells, a propidium iodide solution was added to the cells, and their distribution in the cell cycle phases was analyzed by FACS analysis.

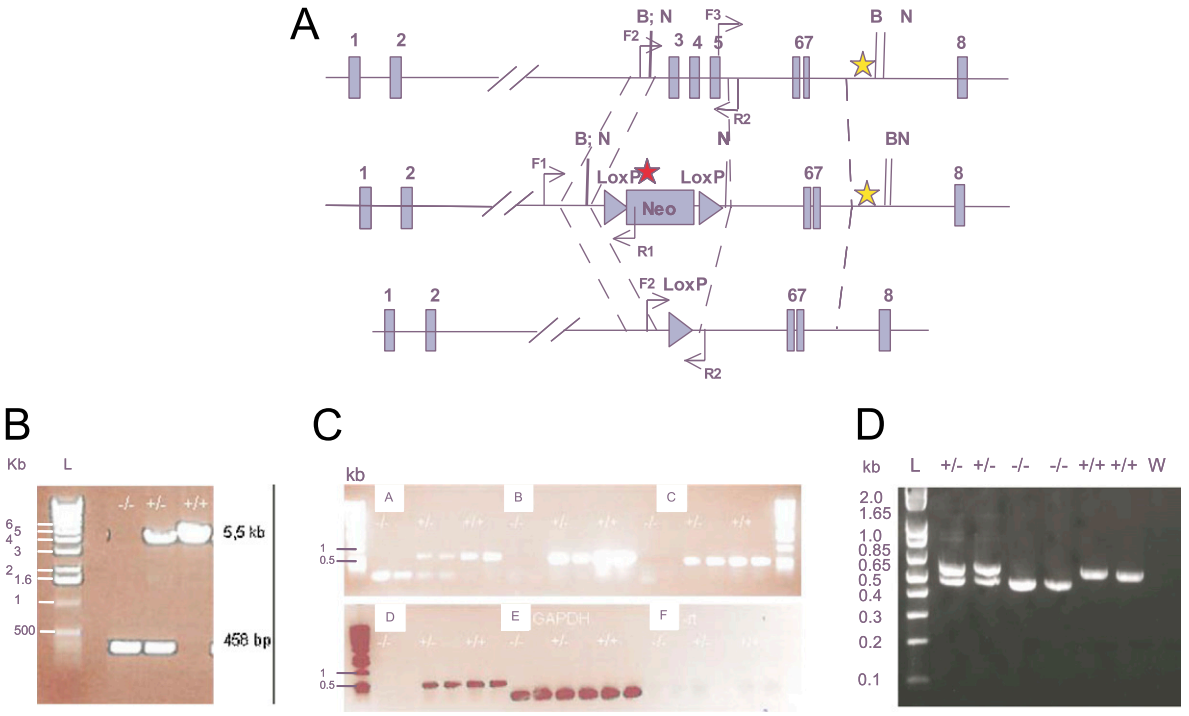

Fig. S3. Design of the targeting construct for the generation of the PGC1α$^{-/-}$ mouse. (*A*) The LoxP collapse results in the deletion of exons 3–5, with a LoxP remnant at the deletion junction of introns 2–5. B, BglII site, N, NheI site; yellow star, LA endogenous probe; red star, position of a Neo Southern probe. Arrows indicate the location of genotyping PCRs. (*B*) Confirmation of the LoxP-Neo collapse and generation of the *Pgc1α* Δex3–5 mice using genomic DNA and PCR primers F2 and R2 (shown in Fig. 1*A*; WT allele, 5.5 kb; Δex3–5 allele, 458 bp). (*C*) RT-PCR on liver cDNA from WT and mice heterozygous and homozygous for the Δex3–5 allele. PCRs were performed using (*A*) Ex2F and Ex6R (WT allele, 700 bp; Δex3–5 allele, 174 bp), (*B*) Ex2F and Ex5R (WT allele, 649 bp; Δex3–5 allele, no band), (*C*) Ex3F and Ex5R (WT allele, 552 bp; Δex3–5 allele, no band), (*D*) Ex3F and Ex5R (WT allele, 501 bp; Δex3–5 allele, no band), (*E*) positive control GAPDH (GAPDHF and GAPDHR, 170 bp), and (*F*) A minus RT GAPDH (GAPDHF and GAPDHR, no band). (*D*) Routine genotyping PCR on tail genomic DNA for the Δex3–5 allele using PCR primers F2, F3, and R2 (WT allele, 539 bp; Δex3–5 allele, 458 bp).

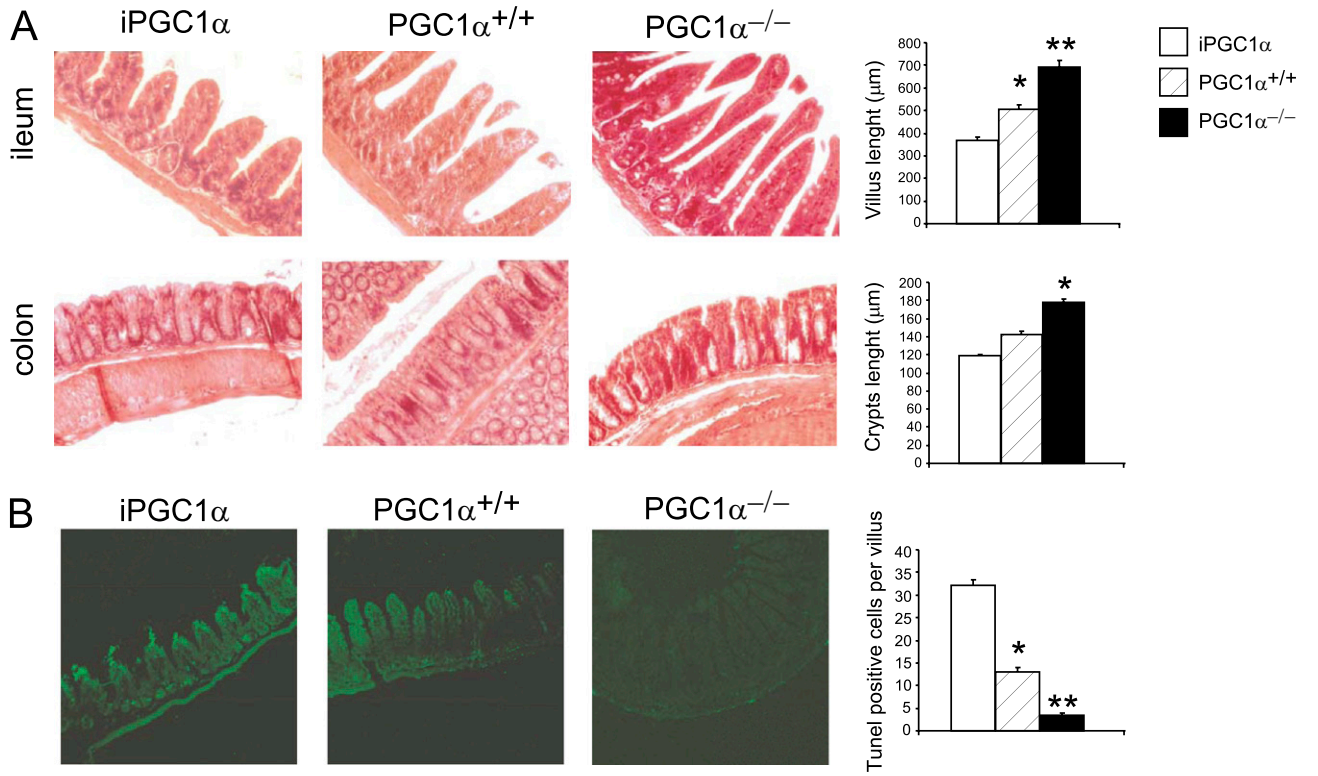

Fig. S4. PGC1α modifies intestinal morphology and enterocyte behavior. (*A*) H&E-stained sections of ileum and colon from iPGC1α, PGC1α$^{+/+}$, and PGC1α$^{-/-}$ mice. Length differences in villi and crypts dimension among the three genotypes are reported in the graphs. (*B*) TUNEL assay on ileum and colon samples from iPGC1α, PGC1α$^{+/+}$, and PGC1α$^{-/-}$ mice. The number of TUNEL-positive cells is reported in the graph.

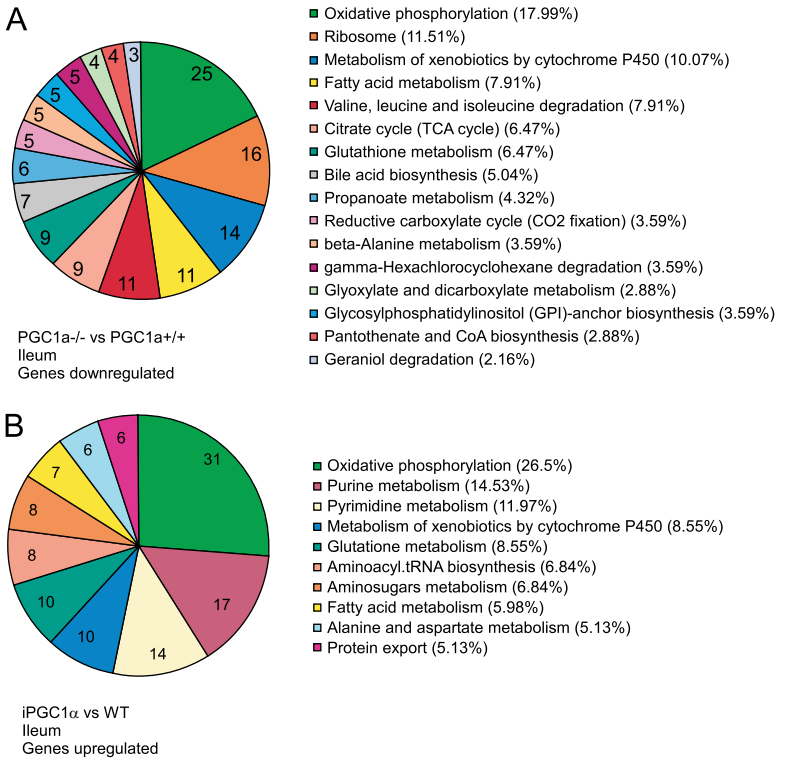

Fig. S5. Microarray analysis of the ileum of iPGC1α, PGC1α$^{+/+}$, and PGC1α$^{-/-}$ mice. Ileum samples from (*A*) PGC1α$^{-/-}$ versus PGC1α$^{+/+}$ and from (*B*) iPGC1α versus PGC1α$^{+/+}$ mice have been analyzed for their gene expression profile by microarray analysis. The metabolic pathways differentially expressed in the three mouse models have been identified using DAVID software on the DAVID Bioinformatics Resources Web site.

Table S1. Differentially expressed proapoptotic genes in intestinal epithelial cells from WT and iPGC1α transgenic mice

Symbol	NCBI accession no.	WT	WT SD	iPGC1α	iPGC1α SD	Fold	Definition
Birc5	NM_009689.2	497.69	36.49	773.92	77.60	0.56	Baculoviral IAP repeat-containing 5, transcript variant 1
Rab1b	NM_029576.1	790.07	6.39	1219.67	91.22	0.54	RAB1B, member RAS oncogene family
Cldn15	NM_021719.3	2572.10	331.94	3732.10	80.87	0.45	Claudin 15
Tradd	NM_001033161.2	849.96	54.65	1193.24	5.47	0.40	TNFRSF1A-associated via death domain
Aifm1	NM_012019.2	460.31	15.95	644.93	25.80	0.40	Apoptosis-inducing factor, mitochondrion-associated 1
Erh	NM_007951.1	1915.07	128.83	2528.21	139.17	0.32	Enhancer of rudimentary homolog (*Drosophila*)
Smarcb1	NM_011418.1	470.21	22.94	613.18	16.12	0.30	SWI/SNF-related, matrix-associated, actin-dependent regulator of chromatin
Jtv1	NM_146165.1	406.90	18.98	508.74	3.09	0.25	JTV1 gene
Caprin1	NM_016739.2	1443.37	8.03	1707.49	15.07	0.18	Cell cycle-associated protein 1
Parp4	XM_994286.2	740.68	5.94	610.40	0.29	−0.18	Poly(ADP ribose) polymerase family, member 4
Prkaa2	NM_178143.1	636.52	8.22	516.27	18.25	−0.19	Protein kinase, AMP-activated, α2 catalytic subunit
Rreb1	NM_001013392.3	1638.40	73.98	1308.38	0.37	−0.20	Ras-responsive element binding protein 1, transcript variant 1
Map3k7ip2	NM_138667.2	1343.12	33.92	1062.16	71.87	−0.21	MAP kinase kinase kinase 7-interacting protein 2
Rassf1	NM_019713.3	1122.18	70.44	880.53	23.37	−0.22	Ras association (RalGDS/AF-6) domain family member 1
Rragc	NM_017475.2	2732.00	83.82	2125.28	13.68	−0.22	Ras-related GTP binding C
Tcf4	NM_013685.2	1204.30	12.28	934.65	61.85	−0.22	Transcription factor 4, transcript variant 1
Nkiras2	NM_028024.2	809.83	13.91	626.42	2.20	−0.23	NF-kB inhibitor-interacting Ras-like protein 2
Il28ra	NM_174851.2	824.79	29.51	633.74	24.19	−0.23	Interleukin 28 receptor alpha
Parp14	NM_001039530.1	3243.40	87.43	2485.66	171.49	−0.23	Poly(ADP ribose) polymerase family, member 14
Tgfbi	NM_009369.1	9423.85	404.38	7145.82	223.95	−0.24	TGF-β induced
Mdm2	NM_010786.2	881.95	41.91	620.80	3.86	−0.30	Transformed mouse 3T3 cell double minute 2
Flcn	NM_146018.1	713.77	23.45	500.94	58.25	−0.30	Folliculin
Dedd2	NM_207677.3	1376.03	18.28	930.99	116.07	−0.32	Death effector domain-containing DNA binding protein 2
Casp4	NM_007609.1	1154.88	12.43	767.72	81.16	−0.34	Caspase 4, apoptosis-related cysteine peptidase
Pcdh1	NM_029357.3	1118.48	109.98	737.45	3.20	−0.34	Protocadherin 1
Ndrg1	NM_008681.2	2653.81	10.03	1592.61	57.12	−0.40	*N*-myc downstream-regulated gene 1

Presented are mean of expression signals with SDs and fold comparisons using WT mice as calibrators.

Table S2. Mean mRNA expression levels with SDs of PPAR-γ and its targets L-FABP, KLF4, and Keratin20 as well as ERRα target VEGF in the intestinal mucosa of WT and iPGC1α mice as measured via real-time qPCR using WT mice as calibrators (*n* = 12)

Symbol	WT	WT SD	iPGC1α	iPGC1α SD	*P*
PPAR-γ	0.8	1.1	1.2	0.5	N.S.
L-FABP	2.5	3.3	49.1	73.7	0.04
KLF4	1	0.1	1.8	0.6	0.0002
Keratin20	0.9	0.1	1.6	0.8	0.06
ERRα	0.9	0.2	1.8	0.7	0.0003
VEGF	0.8	0.1	1.5	0.8	0.06

N.S., not significant.

Table S3. Oligo sequences designed to generate PGC1α$^{-/-}$ mice

Primers PGC1α	Sequence
LA 3′ extraction	5′CAGAAAGCATGGCATTGAATTTCAGTGTGGTAACCAGAAATCCGTTAATC*AGCGTCAGACCCCGTAGAAAA*
SA 5′ extraction	5′AAGTTTGCTACTGTTAGGAACTGTAGATATATGATATACAGGCTATCTGA*TTCTCATGTTTGACAGCTTATCA*
Neo insertion site 5′ exon 3	5′GCCAGCTTCATTAGATGTCAGCAACTTAGGTGAATTTTGTAATAGAATCA**CTCTAGAACTAGTGGATCCG** XbaI SpeI BamHI
Neo insertion site 3′ exon 5	5′GTCAATGATCTCAGTAATCCAGATAAGCCTCAAAGGTATTGTGATCCCAG**GGTATCGATAAAGCTAGCTT** Cla I Nhe I
F1	5′GAGGAGTAGAAGGTGGCGCGAAGG
R1	5′GAGGAGTAGAAGGTGGCGCGAAGG
F2	5′ATAAGGCCCTGCCTAATTTCTCT
R2	5′CGTAATGCTATTTCCTGCTTCTC
F3	5′CAGAGCTTCTCAAGTATCTGACCA
Ex2F	5′CAGATCTTCCTGAACTTGACCTTT
Ex3F	5′AGATGAAGAGAATGAGGCAAACTT
Ex5R	5′GGTTGTGTATGGGACTTCTTTTTC
Ex6R	5′GTCAGAGGAAGAGATAAAGTTGTT
GAPDHF	5′TCCACGACATACTCAGCAC
GAPDHR	5′AACGACCCCTTCATTGAC

In blue (forward) and red (reverse) homologies to pBR328 for amplification of Tet ori sequence. Flanking sequences of Neo cassette are in bold.